Research

Inositol polyphosphates-regulated polyubiquitination of PHR1 by NLA E3 ligase during phosphate starvation response in Arabidopsis

Su-Hyun Park* , Jin Seo Jeong* , Chung-Hao Huang, Bong Soo Park and Nam-Hai Chua

Temasek Life Sciences Laboratory, National University of Singapore, 1 Research Link, Singapore City, 117604, Singapore

Summary

• Phosphate (Pi) availability is a major factor limiting plant growth and development. The key transcription factor controlling Pi-starvation response (PSR) is PHOSPHATE STARVATION RESPONSE 1 (PHR1) whose transcript levels do not change with changes in Pi levels. However, how PHR1 stability is regulated at the post-translational level is relatively unexplored in *Arabidopsis thaliana*.

• Inositol polyphosphates (InsPn) are important signal molecules that promote the association of stand-alone SPX domain proteins with PHR1 to regulate PSR. Here, we show that NITROGEN LIMITATION ADAPTATION (NLA) E3 ligase can associate with PHR1 through its conserved SPX domain and polyubiquitinate PHR1 *in vitro*. The association with PHR1 and its ubiquitination is enhanced by InsP6 but not by InsP5.

• Analysis of InsPn-related mutants and an overexpression plant shows PHR1 levels are more stable in *itpk4-1* and *vih2-4/VIH1^amiRNA* but less stable in *ITPK4* overexpression plants. Under Pi-deficient conditions, *nla* seedlings contain high PHR1 levels, display long root hair and accumulate anthocyanin in shoots phenocopying *PHR1* overexpression plants. By contrast, *NLA* overexpression plants phenocopy *phr1* whose phenotypes are opposite to those of *nla*.

• Our results suggest NLA functions as a negative regulator of Pi response by modulating PHR1 stability and the NLA/PHR1 association depends on InsPn levels.

Introduction

As an essential element for plant growth, phosphorus (P) is required for the synthesis of molecules such as nucleic acids, ATP and phospholipids. Therefore, it is not surprising that phosphate (Pi) deficiency affects plant growth and development and reduces crop yield and productivity (Bieleski, 1973; Schachtman *et al.*, 1998; Hinsinger, 2001). In general, only 10–25% of applied Pi fertilizer is accessible to plants. This low efficiency is largely due to the reaction of Pi with soil components converting it into water-insoluble forms. The overapplication of Pi fertilizers by farmers has led to runoff and environmental pollution (Mitra, 2015; Wang *et al.*, 2016).

During the last two decades, much progress has been on the molecular details underlying responses of Arabidopsis and crops to Pi deficiency. Several transcription factors, such as MYB, WRKY, zinc finger and bHLH, have been implicated in a molecular network regulating Pi-starvation responses (PSR; Franco-Zorrilla *et al.*, 2004; Yi *et al.*, 2005; Devaiah *et al.*, 2007; Chen *et al.*, 2009; Su *et al.*, 2015). Among these, PHOSPHATE STARVATION RESPONSE 1 (PHR1), a MYB transcription

factor, has emerged as a key factor in coordinating PSR (Rubio *et al.*, 2001; Bustos *et al.*, 2010). Under Pi-deficient conditions, PHR1 binds to PHR1-binding sequence on the promoters of PSR genes such as *IPS1* (Martín *et al.*, 2000), *pri-miR399* (Aung *et al.*, 2006; Bari *et al.*, 2006) and *pri-miR827* (Wang *et al.*, 2012) to control PSR gene expression (Rubio *et al.*, 2001; Bustos *et al.*, 2010; Lv *et al.*, 2014; Wang *et al.*, 2014). Arabidopsis plants overexpressing PHR1 accumulate higher Pi levels in shoots than wild-type (WT; Nilsson *et al.*, 2007), whereas *phr1* showed defective accumulation of anthocyanin and lack of root hair growth under Pi-starvation conditions (Bustos *et al.*, 2010). Orthologs of PHR1 have been identified in *Brassica napus* (Ren *et al.*, 2012), rice (Zhou *et al.*, 2008) and wheat (Wang *et al.*, 2013). In both Arabidopsis and rice, PHR1 and PHR1-like transcription factors show functional redundancy, and they are able to form homodimers and heterodimers (Bustos *et al.*, 2010; Guo *et al.*, 2015; Sun *et al.*, 2016; Ruan *et al.*, 2017). Among PHR1 and homologues, PHR1 and PHL2 are the key factors regulating the accessibility of chromatin of PSR genes under Pi-limited conditions (Barragán-Rosillo *et al.*, 2021).

Arabidopsis and rice contain 4 (*AtSPX1–SPX4*) and 6 (*OsSPX1–OsSPX6*) SPX genes, respectively. These genes, which encode stand-alone SPX proteins, are expressed in roots, leaves,

---

*These authors contributed equally to this work.

cotyledons, stems and pollen grains, and most of them, except AtSPX4 and OsSPX4, are induced by Pi starvation. Stand-alone SPX proteins have been shown to function as inhibitors of PHR1 and its homologues. Under Pi-sufficient conditions, SPX proteins interact with PHR1 to restrain it from binding to PSR gene promoters (Wang *et al.*, 2009, 2014; Lv *et al.*, 2014; Puga *et al.*, 2014). In addition to *SPX* genes, there are three other *SPX*-related gene subfamilies encoding SPX-EXS, SPX-MFS and SPX-RING depending on the additional domain on their C-terminus. As a member of the SPX-EXS subfamily, PHO1 is involved in long-distance Pi transfer (Stefanovic *et al.*, 2007). Phosphate transporters such as PHOSPHATE TRANSPORTER 5 or VACUOLAR PHOSPHATE TRANSPORTER, which belong to the SPX-MFS subfamily, regulate cytoplasmic Pi homeostasis (Liu *et al.*, 2016). The third subfamily consists of SPX proteins with a RING domain, which endows E3 ubiquitin ligase activity. An example is the Arabidopsis NITROGEN LIMITATION ADAPTATION (NLA), which has been shown to target the Pi transporter PHT1 for degradation by 26S proteasomes (Park *et al.*, 2014). On the contrary, SKP1–CULLIN–F-Box protein complex promotes PHR1 degradation to repress *PHT1;1* expression in the presence of arsenate under low Pi conditions (Navarro *et al.*, 2021; Kandhol *et al.*, 2022). Recently, Guo *et al.* (2022) reported that iron sensors, OsHRZ1 and OsHRZ2 RING-domain proteins, function as negative regulators by ubiquitinating OsPHR2 to fine-tune Pi/iron signalling and homeostasis in rice.

Inositol polyphosphates (InsPn) are important small signalling molecules in plants required to maintain normal functions of plant development and for responses to multiple stresses (Tsui & York, 2010). In the last several years, InsPn have been shown to play important roles in PSR by modulating the association of transcription factors with SPX-containing proteins. Wild *et al.* (2016) first showed InsP6 and InsP7 promote interaction between OsSPX4 and OsPHR2 with a Kd of 7–50 μM. Subsequently, InsP8 was found to directly bind to the SPX domain of SPX1 and is essential for SPX1/PHR1 interaction (Dong *et al.*, 2019; Zhu *et al.*, 2019). Recent crystallographic study identified the MYB coiled-coil domain in PHRs as a target of InsP8–SPX complex. Binding of the InsP8–SPX complex to PHR1 prevents the latter from accessing PSR gene promoters (Ried *et al.*, 2021). Inositol polyphosphates are synthesized in cells through the action of a kinase cascade. InsP6, which is produced from InsP5 by inositol pentakisphosphate 2-kinase, can be phosphorylated by the inositol hexakisphosphate kinases to form InsP7. The latter can be further phosphorylated by diphosphoinositol pentakisphosphate kinase (PPIP5K) to produce InsP8 (Cridland & Gillaspy, 2020). The Arabidopsis genome encodes four inositol 1,3,4-trisphosphate 5/6-kinase (ITPK) genes, namely *ITPK1*, *ITPK2*, *ITPK3* and *ITPK4*, that are responsible for the conversion of InsP3 to InsPn. Under Pi-replete conditions, the mutants, *ipk1*, *itpk1* and *itpk4*, show reduced levels of InsP7 and InsP8 but elevated levels of PSR gene transcripts compared with WT (Kuo *et al.*, 2014, 2018). In addition to the ITPK kinases, Arabidopsis also expresses two homologous PPIP5K, VIH1 and VIH2, that function in InsP8 biosynthesis

by converting InsP7 to InsP8 (Dong *et al.*, 2019; Zhu *et al.*, 2019). Plants of the InsP8-deficient *vih1/vih2* double mutant exhibit constitutive PSR leading to Pi accumulation (Dong *et al.*, 2019; Zhu *et al.*, 2019). The phenotype of the *vih1/vih2* double mutant can be reversed in the quadruple mutant, *vih1/vih2/phr1/phl1*, indicating that PHR1 and its homologue PHL1 mediate the PSR (Zhu *et al.*, 2019). The lack of InsP8 in the *vih1/vih2* mutant attenuates the SPX1-PHR1 interaction found in WT (Dong *et al.*, 2019; Ried *et al.*, 2021).

Although PHR1 is a key transcription factor for PSR, it is striking that *PHR1* transcript levels remain unchanged upon Pi depletion (Rubio *et al.*, 2001; Bustos *et al.*, 2010), suggesting major regulation of this factor occurs at a post-translational level. Here, we identified NLA, an SPX-containing E3 ligase, as a negative, post-translational regulator of PHR1. We showed that NLA could ubiquitinate PHR1 *in vitro* and *in vivo* to accelerate PHR1 protein decay. Inositol polyphosphates facilitate NLA/PHR1 interaction and promote PHR1 destruction. Seedlings of *nla* display long root hair and accumulation of anthocyanin in shoots under Pi-deficient conditions phenocopying *PHR1* overexpressing plants. On the contrary, *NLA* overexpressing plants share the same Pi response phenotype as *phr1* mutant. Our findings uncover NLA as a negative regulator of PHR1 under diverse Pi conditions.

Materials and Methods

Plant materials and growth conditions

Arabidopsis thaliana L. (ecotype Col-0) was used as the WT, and all mutants and transgenic lines were generated in this background. Seeds were germinated on 0.8% agar medium containing Murashige and Skoog (MS) salt and 1% sucrose. Plants were grown on medium in a growth chamber at 22°C in long-day conditions (16 h : 8 h, light : dark) under LED light at 100 μmol m^{-2} s^{-1}. T-DNA insertion mutants, *nla* (CS858095), *phr1* (SALK_067629) and *itpk4-1* (SAIL_33_G08) and overexpression lines *35S:NLA-6MYC* (Park *et al.*, 2018) were used in this study. The *phr1/nla* double mutant was generated by genetic crossing. *vih2-4/VIH1^{amiRNA}* (CS2109987; ABRC, Columbus, OH, USA) plants were obtained by transforming *vih2-4* mutant plants with a β-oestradiol-inducible amiRNA construct targeting *VIH1* (Zhu *et al.*, 2019).

Plasmid DNA constructions

Full-length cDNA of *PHR1*, and *ITPK4* were isolated by PCR to generate overexpression plants, *UBQ10:PHR1-HA* and *35S:ITPK4-GFP*, respectively. All constructs were transformed into *Agrobacterium tumefaciens* strain GV3101, which was used for transformation by the floral dip transformation method (Clough & Bent, 1998; Zhang *et al.*, 2006).

Anthocyanin content quantification

Leaf tissues of plants grown on Pi-deficient (−P) and Pi-sufficient (+P) media were frozen with liquid nitrogen and

ground into a powder using a mortar and pestle. The powder was resuspended into 10 volumes (based on fresh weight) of 45% methanol and 5% acetic acid. After centrifugation at 12 000 g for 10 min, the absorbance of the supernatant at 530 and 657 nm was measured and the anthocyanin content (abs_{530}/g FW) was calculated by $(abs_{530} - (0.25 \times abs_{657})) \times 10$ (Laby et al., 2000).

In vitro pull-down assays

pGST-PHR1, pMBP-NLA, pMBP-SPX domain, pMBP-RING domain, pMBP and pMBP-PHR1 were transformed into *Escherichia coli* BL21. Recombinant proteins were expressed by induction using 1 mM isopropyl-β-D-thiogalactoside at 22°C for 12 h. Recombinant protein purification and *in vitro* protein binding assays were performed as described by Park et al. (2019). GST resin-bound proteins GST-PHR1 were individually incubated with MBP-NLA, MBP-SPX domain, MBP-RING domain, MBP or MBP-PHR1 in 1 ml of pull-down buffer (50 mM Tris–HCl, pH 7.5, 200 mM NaCl, 0.5% Triton X-100, 0.5 mM β-mercaptoethanol and proteinase inhibitor cocktail) at 25°C for 2 h. After incubation, mixtures were washed five times with pull-down buffer. Pulled-down proteins were analysed on 8% SDS-PAGE and detected with anti-MBP antibody (15089-1-AP; Proteintech, Rosemont, IL, USA) by immunoblotting. To test the association between PHR1 and NLA or SPX domain with different concentrations of InsP6, 1 µg of GST resin-bound GST-PHR1 was mixed with 2 µg of MBP-NLA or MBP-SPX domain, and different amounts (10–40 µM) of InsP6 (P8810; Sigma) or InsP5 (5-0-13 456-Na; SiChem, Bremen, Germany). The mixtures were incubated at 30°C for 4 h and washed five times with pull-down buffer. Residual MBP-NLA or MBP-SPX domain associated with GST-PHR1 were detected by anti-MBP antibody. Anti-rabbit IgG horseradish peroxidase (HRP)-linked whole antibody from donkey was used as the secondary antibody (1 : 10 000 dilution; NA934; Cytiva, Malborough, MA, USA). An ECL Prime Western Blotting System (RPN2232; Cytiva) and iBright Imaging System (Invitrogen) were used for detection.

In vivo co-immunoprecipitation assays

UBQ10:PHR1-HA and *35S:NLA-myc* seedlings were grown on MS medium for 10 d and then treated with 50 µM MG132 for 16 h at 22°C. Co-immunoprecipitation assays (Co-IP) were performed as described by Park et al. (2022). Homogenized samples were incubated in 1 ml Co-IP buffer (50 mM Tris–HCl, pH 7.5, 100 mM NaCl, 10 mM MgCl₂, 0.1% Nonidet P-40, 1 mM PMSF, 10% glycerol, 1 mM DTT, 50 µM MG132 and protease inhibitor cocktail) for 1 h at 4°C. Total protein extracts were precleared for 1 h at 4°C by adding protein A agarose, and an aliquot was reserved as the input sample. The precleared protein extracts were incubated with anti-HA (SC-805; Santa Cruz, Dallas, TX, USA), anti-myc (SC-40; Santa Cruz) or without any antibody (−Ab) for 2 h at 4°C. Antigen–antibody complexes were pulled down by protein A agarose for 1 h at 4°C and washed four times with Co-IP buffer. The immunoprecipitated proteins

were separated on 8% SDS-PAGE for PHR1-HA and PHR1 and 10% SDS-PAGE for NLA-myc and NLA. The proteins were detected by anti-HA, anti-myc, anti-PHR1 or anti-NLA using anti-PHR1 and anti-NLA antibodies produced in rabbits. N-terminal PHR1 (PHR1-N, Supporting Information Fig. S1) and full-length NLA proteins were purified by His-tag and used as immunogens, separately. For secondary antibodies, anti-mouse IgG HRP-linked whole antibody from sheep (1 : 5000 dilution; NA931; Cytiva) was used to detect PHR1-HA and anti-rabbit IgG HRP-linked whole antibody from donkey (1 : 5000 dilution; NA934; Cytiva) was used to detect PHR1, NLA and NLA-myc proteins. An ECL Prime Western Blotting System (RPN2232; Cytiva) and iBright Imaging System (Invitrogen) were used for detection.

Bimolecular fluorescence complementation assays

35S:nYFP-NLA, *35S:PHR1-cYFP*, *35S:NLA-YFP*, *35S:PHR1-YFP*, *35S:mCherry-NLS*, *35S:P19* and YFP empty vector controls were transformed into *Agrobacterium* (GV3101). Cultured agrobacterial cells with all constructs were incubated in an infiltration solution (10 mM MgCl₂, 150 µM acetosyringone) at 25°C for 3 h without shaking and then infiltrated into leaves of *Nicotiana benthamiana*. Images were observed using an SP8 laser scanning confocal microscope (Leica) 3 d after infiltration.

In vitro ubiquitination assays

In vitro ubiquitination reactions were performed as described by Park et al. (2022). Five hundred ng of MBP-PHR1-myc was reacted with 100 ng UBE1 (E1; E-304; BostonBiochem, Cambridge, MA, USA), 100 ng of UbcH6 (E2; E2-622; BostonBiochem) or 100 ng of purified GST-PHO2, 500 ng of MBP-NLA-HA (E3) and 2 µg His-Ubiquitin (U5507; Sigma-Aldrich) in ubiquitination buffer (50 mM Tris pH 7.4, 5 mM MgCl₂, 2 mM dithiothreitol, 5 mM ATP and 100 µM ZnCl₂) for 4 h at 30°C. To investigate ubiquitination patterns of PHR1 with different amounts of InsPn, the same amount of E1, E2, E3 and substrate used in reactions as described previously and added different concentrations of InsP6 or InsP5 for 4 h at 30°C. After separation on 6% SDS-PAGE, the proteins were detected by anti-myc antibody (16286-1-AP; Proteintech). Anti-rabbit IgG HRP-linked whole antibody from donkey was used as the secondary antibody (NA934; 1 : 10 000 dilution; Cytiva). An ECL Prime Western Blotting System (RPN2232; Cytiva) and iBright Imaging System (Invitrogen) were used for detection.

PHR1 stability assays

Ten-day-old seedlings of WT, *itpk4-1* and *35S:IPTK4-GFP* were treated with 200 µM cycloheximide (C1988; Sigma-Aldrich). Seedlings were collected at different time points. After being frozen in liquid nitrogen, seedlings were homogenized into a powder with a mortar and pestle. The powder was dissolved in two volumes of protein extraction buffer (same as the Co-IP buffer; 50 mM Tris–HCl, pH 7.5, 100 mM NaCl, 10 mM MgCl₂, 0.1% Nonidet

P-40, 1 mM PMSF, 10% glycerol, 1 mM DTT, 50 μM MG132 and protease inhibitor cocktail). The extracts were centrifuged at 12 000 g for 10 min at 4°C, and soluble proteins were separated on 8% SDS-PAGE and detected by anti-PHR1 and anti-β-actin antibodies (66009-1-Ig; Proteintech). β-Actin levels were used as a loading control. For the secondary antibody, an anti-rabbit IgG HRP-linked whole antibody from donkey (1 : 5000 dilution; NA934; Cytiva) was used to detect PHR1 protein. Anti-mouse IgG HRP-linked whole antibody from sheep (1 : 5000 dilution; NA931; Cytiva) was used to detect β-actin. An ECL Prime Western Blotting System (RPN2232; Cytiva) and iBright Imaging System (Invitrogen) were used for detection. All assays were repeated in three independent experiments. The intensity of Western blot bands was measured using the NIH IMAGEJ software.

Phenotype assays

Sterilized seeds were incubated for 3 d at 4°C in the dark and then germinated on 0.8% MS medium with 1% sucrose. Seedlings grown for indicative days were transferred to 1.4% agar MGRL (Fujiwara *et al.*, 1992) with 1% sucrose and modified MGRL containing 1.75 mM MES (pH 5.8) instead of 1.75 mM sodium Pi (pH 5.8) and grown for 7 d in long-day conditions (16-h : 8-h, light : dark) under LED light at 100 μmol m^{-2} s^{-1}. Root hair phenotype was observed with a stereomicroscope (SMZ25; Nikon, Minato City, Japan).

Real-time qRT-PCR analysis

Total RNA was extracted from whole seedlings using Trizol (15596026; Invitrogen) and purified using Easy Pure Plant RNA Kit (74104; Qiagen) after DNase I (79254; Qiagen) treatment. Reverse transcription was performed using 2 μg of each total RNA (K1622; Thermo Scientific, Waltham, MA, USA). qPCR was performed using SYBR premix (172-5275; Bio-Rad) on the CFX96 (Bio-Rad). All qRT-PCR experiments were performed with three technical replicates. Transcript levels were normalized to *ACT2* expression levels. Primers used are listed in Table S1.

Results

nla phenocopies PHR1^{OX} whereas *phr1* phenocopies NLA^{OX}

Wild-type, *nla*, *phr1* and *phr1/nla* plants were grown on MS medium for 10 d and then transferred to +P (Pi-sufficient) or −P (Pi-deficient) medium. After 7 d, root hair length of *nla* seedlings on −P media was 1.81 times longer, whereas those of *phr1* seedlings were 0.68 times shorter compared with WT seedlings (Fig. 1a). In addition, anthocyanin levels in *nla* shoots were 1.56 times higher, whereas those of *phr1* were 0.58 times lower than in WT (Fig. 1b). There was little difference in the plant stature among the various genotypes. The root hair phenotype and anthocyanin accumulation in *nla* were abolished in the double

mutant, *phr1/nla*, which was phenotypically similar to *phr1* (Fig. 1a,b). This epistatic effect suggested that NLA and PHR1 operate in the same PSR pathway and that PHR1 functions downstream of NLA.

To complement and strengthen the mutant results, we analysed overexpression lines of *UBQ10:PHR1-HA* (*PHR1^{OX}*) and *35S: NLA-myc* (*NLA^{OX}*) (Park *et al.*, 2018). Consistent with the major role of PHR1 in PSR, *PHR1^{OX}* seedlings showed increased root hair length under +P conditions and the root hair length was further increased under −P conditions, approximately twofold compared with WT (Fig. 2a). Anthocyanin levels were also 1.56 times higher in *PHR1^{OX}* shoots, and the leaf size was smaller than of WT under −P conditions (Fig. 2b). These phenotypes were similar to those of *nla* seedlings under −P conditions except that the *PHR1^{OX}* shoots were smaller than those of WT and *nla* mutant. By contrast, *NLA^{OX}* seedlings produced short root hair compared with WT and anthocyanin levels were reduced in shoots under −P conditions phenocopying *phr1* seedlings (Figs 1, 2).

We analysed the expression of several PSR genes, *IPS1*, *AT4*, *pri-miR827*, *pri-miR399d* and *anthocyanidin synthase* (*ANS*) in various genotypes under −P conditions. Compared with WT, expression levels of PSR genes were highly increased in *nla* and *PHR1^{OX}* plants but lower in *phr1* and *NLA^{OX}* plants (Figs 1c, 2c). Notably, the higher expression of PSR-related genes in *nla* was abolished in the double mutant *phr1/nla* (Fig. 1c), indicating the dependence of these genes on PHR1 activity. In contrast to *nla* mutant, expression levels of these genes in *PHR1^{OX}* were already moderately elevated under +P conditions and further induced under −P conditions. In parallel with the observed phenotype, expression levels of the same genes in *NLA^{OX}* under −P conditions were significantly reduced compared with WT (Fig. 2c). These results suggest NLA may regulate PHR1 depending on Pi levels in the medium.
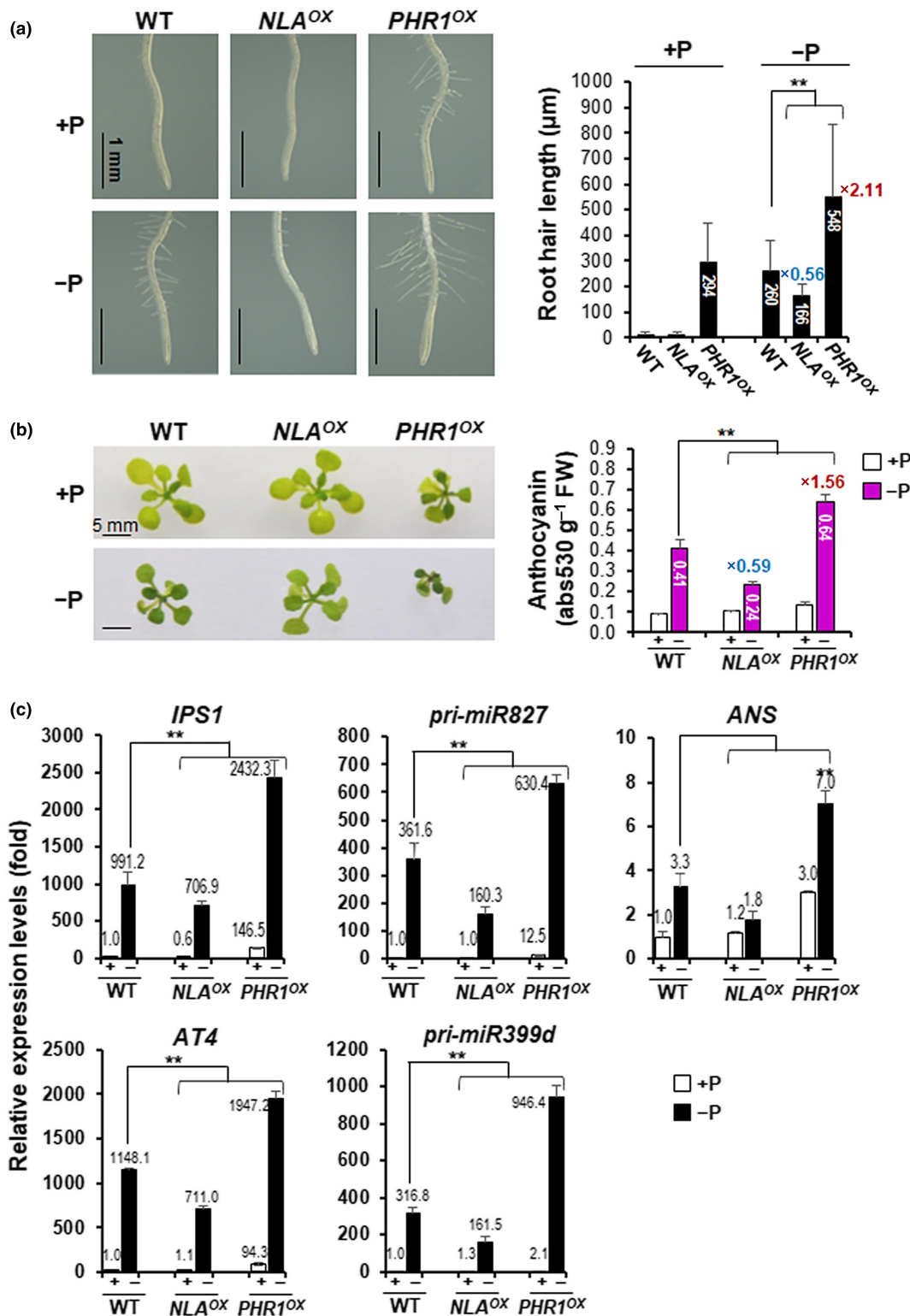
PHR1 associates with NLA *in vitro* and *in vivo*

The genetic relationship between *NLA* and *PHR1* suggested a possible biochemical connection between the two encoded proteins. We raised anti-PHR1 antibody in rabbits using an N-terminal PHR1 fragment (PHR1-N, 1–224 amino acid) as an immunogen (Fig. S1). By *in vitro* pull-down experiments, we explored possible NLA/PHR1 interaction. A previous report showed SPX proteins which consist of a stand-alone SPX domain interact with PHR1 (Puga *et al.*, 2014). NITROGEN LIMITATION ADAPTATION is comprised of an N-terminal region containing an SPX domain and a C-terminal region containing a RING domain, which is required for ubiquitin E3 ligase activity (Fig. 3a). Fig. 3(a) shows that NLA was indeed able to bind to PHR1 *in vitro* and that only the N-terminal region which contains the SPX domain was needed for this association. This result suggested that PHR1 may be a target of NLA ubiquitin E3 ligase.

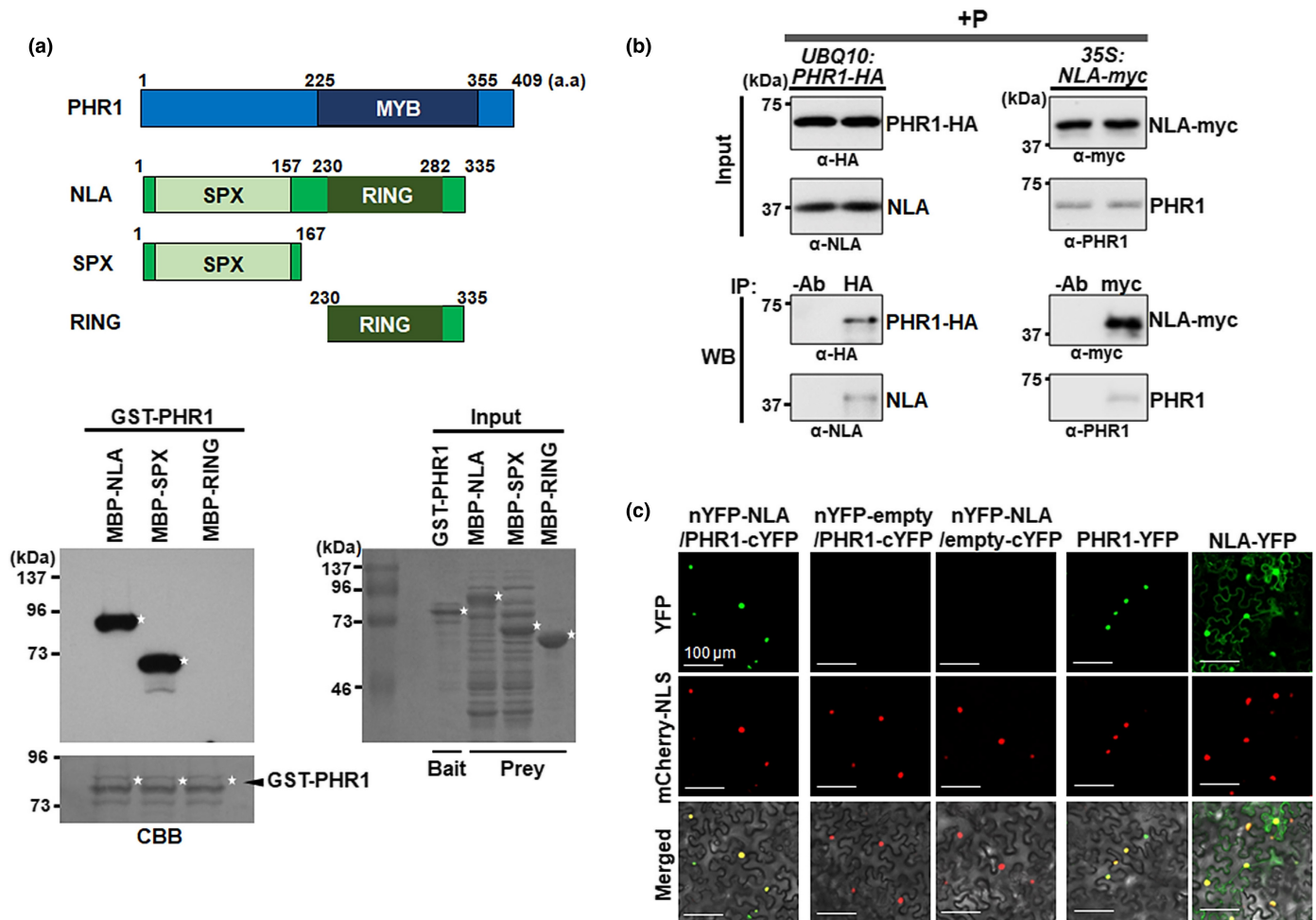To see whether PHR1 may directly associate with NLA *in vivo*, we used seedlings expressing *UBQ10:PHR1-HA* and *35S: NLA-myc* for Co-IP experiments (Fig. 3b). Ten-day-old seedlings were grown on +P medium for another 7 d. Because of the E3
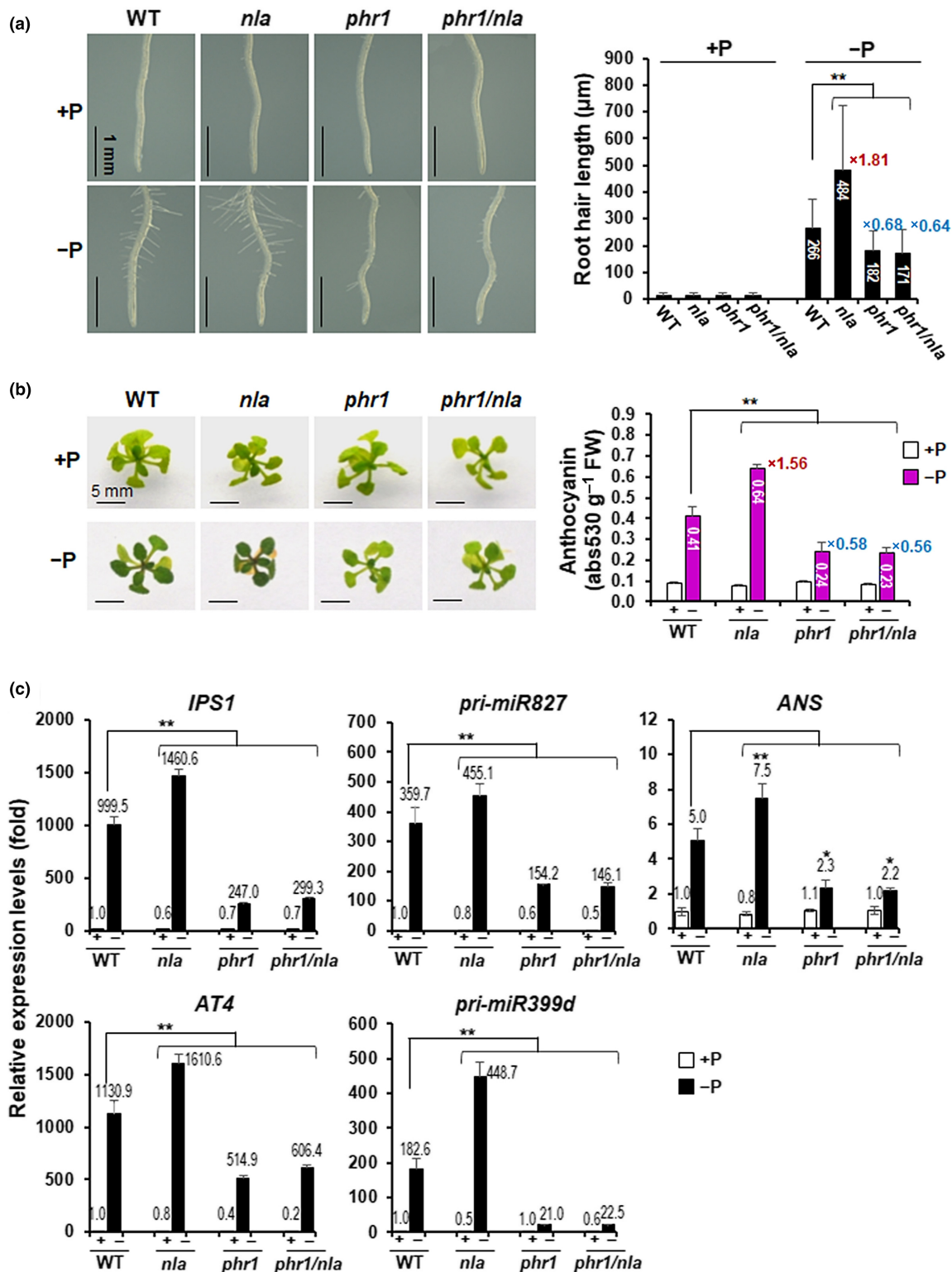
Fig. 1 Responses of *nla*, *phr1* and *phr1/nla* mutants to phosphate (Pi) starvation. Ten-day-old seedlings grown on Murashige and Skoog medium were transferred to Pi deficiency (−P) and Pi sufficiency (+P) media for 7 d. (a) Root hair morphology of primary root of wild-type (WT), *nla*, *phr1* and *phr1/nla* on +P and −P media. Bar, 1 mm. Root hair lengths in the 2 mm region distal from the root tip were measured in 30 roots from each genotype (right panel). Bars represent average values ±SD ($n = 30$). (b) Anthocyanin accumulation in shoots of various genotypes on +P and −P media. Bar, 5 mm. Bars on the right panel are average values ±SD ($n = 3$, independent biological replicates). FW, fresh weight. (c) RT-qPCR analysis of expression of Pi-starvation response genes, *IPS1*, *AT4*, *pri-miR827*, *pri-miR399d* and *anthocyanidin synthase* (*ANS*), in various genotypes grown on +P and −P media. RNAs were extracted from seedlings in (a) and (b). Transcript levels were normalized to *ACT2* levels. Bars are average values ±SD ($n = 3$, independent biological replicates). Asterisks indicate a statistically significant difference compared with WT. **, $P < 0.01$; *, $P < 0.05$; two-tailed *t*-test.

Fig. 2 Responses of NLA^{OX} and $PHR1^{OX}$ to phosphate (Pi) starvation. Ten-day-old seedlings wild-type (WT), NLA^{OX} and $PHR1^{OX}$ on Murashige and Skoog medium were transferred onto Pi deficiency (−P) and Pi sufficiency (+P) media for 7 d. (a) Root hair morphology of primary root seedlings of WT, NLA^{OX} and $PHR1^{OX}$ on +P and −P media. Bar, 1 mm. Root hair lengths in the 2-mm region distal from the root tip were measured in 30 roots from each genotype (right panel). Bars represent average values ±SD ($n = 30$). (b) Anthocyanin accumulation in shoots of various genotypes on +P and −P media. Bar, 5 mm. Bars on the right panel are average values ±SD ($n = 3$, independent biological replicates). FW, fresh weight. (c) RT-qPCR analysis of expression of Pi-starvation response genes, $IPS1$, $AT4$, $pri-miR827$, $pri-miR399d$ and anthocyanidin synthase (ANS), in various genotypes grown on +P and −P media. RNAs were extracted from seedlings in (a) and (b). Transcript levels were normalized to $ACT2$ levels. Bars are average values ±SD ($n = 3$, independent biological replicates). Asterisks indicate a statistically significant difference compared with WT. **, $P < 0.01$; *, $P < 0.05$; two-tailed t-test.

Fig. 3 PHOSPHATE STARVATION RESPONSE 1 (PHR1) associates with NITROGEN LIMITATION ADAPTATION (NLA). (a) Schematic diagrams of PHR1, NLA and NLA derivatives. Numbers indicate amino acid residue (upper panel). NLA and SPX domain of NLA interact with PHR1 *in vitro* (lower panel). Full-length PHR1 was used as a bait, and full-length NLA, N-terminal fragment of NLA (SPX, amino acids 1–167) and C-terminal fragment of NLA (RING, amino acids 230–335) were used as prey for *in vitro* pull-down assays. Left panel, immunoblot; Right panel, input protein amount; CBB, Coomassie blue staining of the blot. Asterisks indicate the full-length version of each protein. (b) PHR1 interacts with NLA in Arabidopsis. Extracts prepared from 10-d-old seedlings carrying *UBQ10:PHR1-HA* and *35S:NLA-myc* treated for 16 h with 50 μM MG132 were used for immunoprecipitation. Left panel: Immunopre-cipitates obtained with anti-HA antibody were tested for the presence of NLA-myc and NLA using anti-myc and anti-NLA antibodies. Right panel: Immunoprecipitates obtained with anti-myc antibody were tested for the presence of PHR1-HA and PHR1 using anti-HA and anti-PHR1 antibodies. IP, immunoprecipitation; WB, western blots; −Ab, no antibody. (c) Bimolecular fluorescence complementation analysis of the association between PHR1 and NLA in *Nicotiana benthamiana*. YFP signals were detected in nuclei of leaf cells when NLA-nYFP was co-expressed with PHR1-cYFP. mCherry-NLS was used to mark the nuclei. Confocal images were taken 3 d after infiltration. Localization is shown by merging mCherry, YFP, and differential interference contrast images (Merged). Bar, 100 μm.
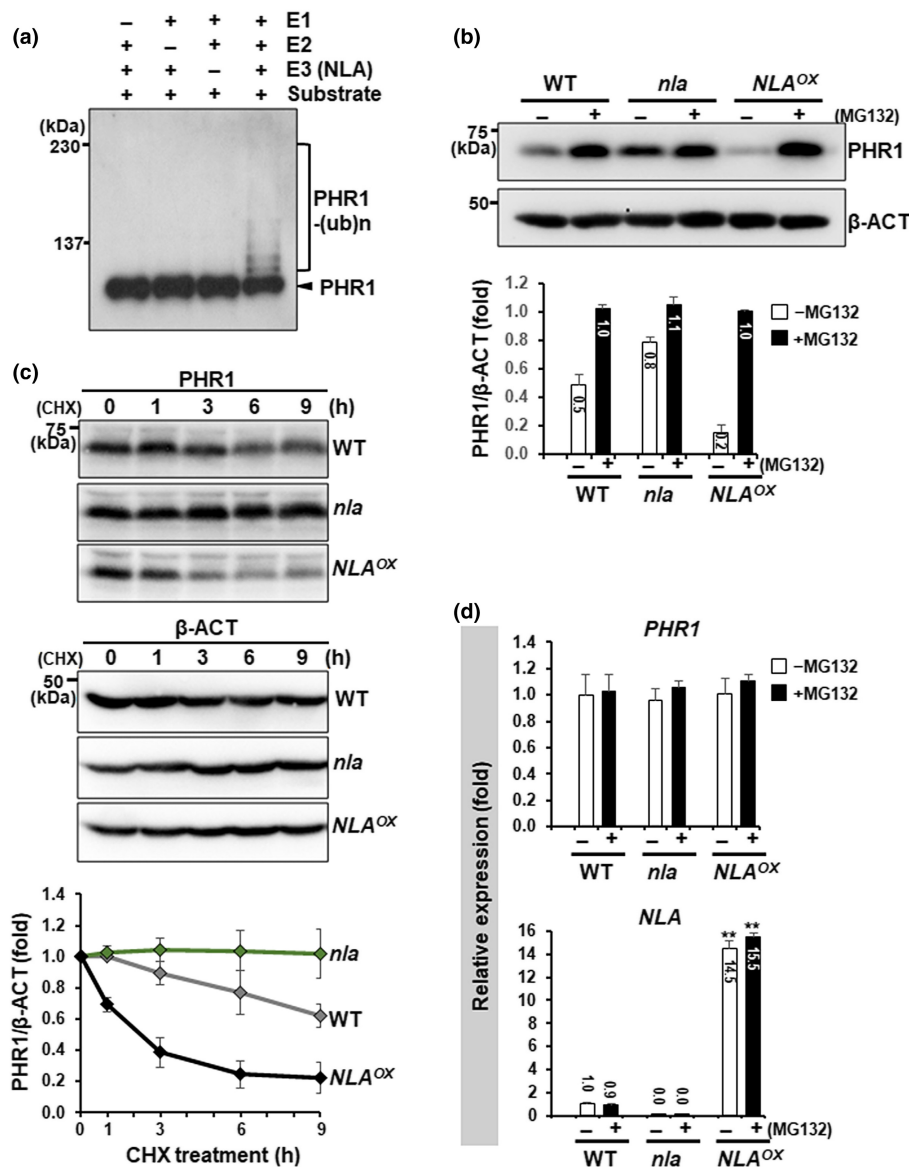
ubiquitin ligase activity of NLA (Park *et al.*, 2014), we treated the seedlings with MG132 to block possible PHR1 degradation. Fig. 3(b) shows that when PHR1-HA and NLA-myc were pulled down using anti-HA and anti-myc antibodies, the immunopre-cipitates also contained NLA-myc (NLA) and PHR1-HA (PHR1), respectively, providing evidence for their *in vivo* interaction.

Next, we used bimolecular fluorescence complementation to determine the subcellular localization of the PHR1/NLA complex. YFP signals of PHR1-YFP were detected in the nucleus, whereas NLA-YFP signals were distributed in both the nucleus and the cytosol (Fig. 3c). We observed that nYFP-NLA was able to associate with PHR1-cYFP, and the PHR1/NLA complex was

localized in the nucleus. No signal was detected with nYFP-empty/PHR1-cYFP and nYFP-NLA/empty-cYFP. Collectively, these results support the view that PHR1 directly associates with NLA in the nucleus.

PHR1 stability is regulated by NLA

To see whether PHR1 is a target of NLA, we performed *in vitro* ubiquitination assays using purified PHR1 as a substrate and NLA as the E3 ligase. Fig. 4(a) shows that PHR1 was indeed polyubiquitinated by NLA *in vitro*. Moreover, PHO2 was active as an E2 in conjunction with the NLA E3 ligase to mediate PHR1 ubiquitination (Fig. S2). If PHR1 is also targeted by NLA
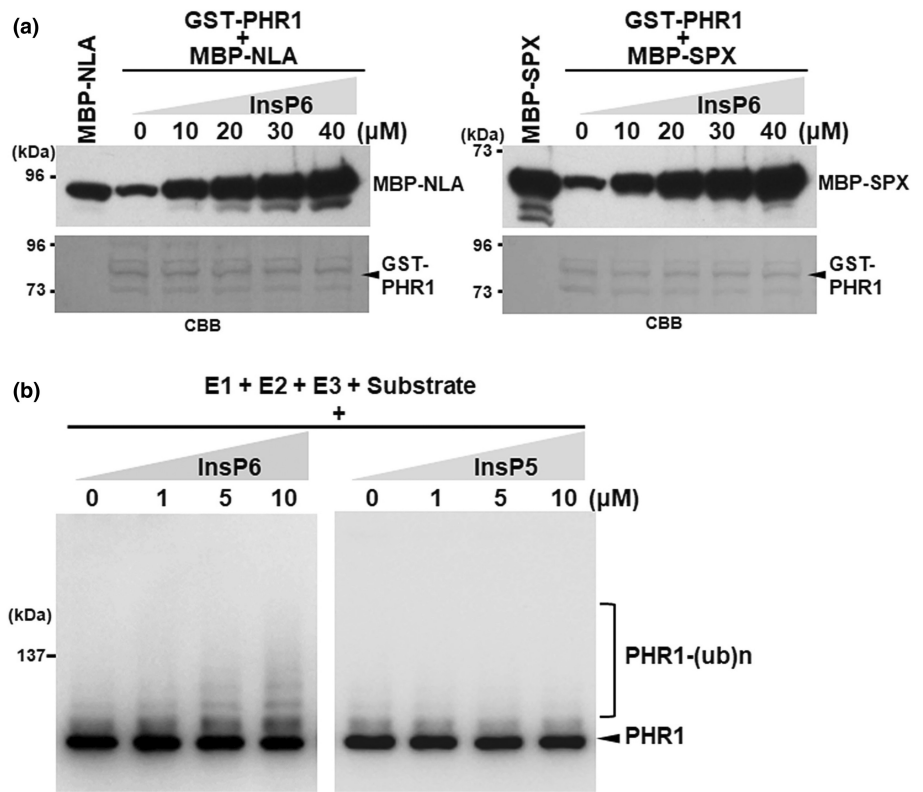
Fig. 4 PHOSPHATE STARVATION RESPONSE 1 (PHR1) is ubiquitinated by NITROGEN LIMITATION ADAPTATION (NLA). (a) PHR1 is ubiquitinated by NLA. Yeast UBE1 (E1), human UBCH6E1 (E2), and purified MBP-NLA (E3) and MBP-PHR1 were used for *in vitro* ubiquitination assay. Polyubiquitinated PHR1 was detected by anti-myc antibody. kDa, kiloDaltons. (b, c) NLA destabilizes PHR1 protein in Arabidopsis. (b) Ten-day-old seedlings of WT, *nla* and *NLA^OX^* were incubated in liquid Murashige & Skoog (MS) medium with or without MG132 (50 μM) for 16 h, and extracts were analysed for PHR1 levels. β-actin levels were used as a loading control, and the intensity of the PHR1 protein bands was measured using IMAGEJ and normalized by β-actin levels. Value in WT sample treated with MG132 was set as 1. (c) Ten-day-old seedlings of WT, *nla* and *NLA^OX^* were treated in liquid MS medium with 200 μM cycloheximide (CHX). Proteins were extracted at indicated times and analysed by immunoblots using anti-PHR1 and anti-β-actin antibodies. β-actin levels were used as a loading control, and the intensity of the PHR1 protein bands was measured using IMAGEJ and normalized by β-actin levels. Values of all three samples at 0 time were set as 1. Plots are average values ±SD (*n* = 3, independent biological replicates). (d) Analysis of *PHR1* and *NLA* transcript levels in (b). Transcript levels were analysed by qRT-PCR and normalized to *ACT2* levels. Bars represent average values ±SD (*n* = 3, independent biological replicates). Asterisks indicate a statistically significant difference compared with WT. **, *P* < 0.01; two-tailed *t*-test.

E3 ligase *in vivo*, its stability should be affected by different NLA levels. We manipulated NLA levels using *nla* mutant and *NLA^OX^* plants and examined PHR1 levels and its stability. Compared with WT, PHR1 protein levels in *NLA^OX^* plants were very low in untreated samples but could be substantially elevated when protein degradation was blocked by MG132 (Fig. 4b). The ratio of PHR1 levels with and without MG132 in *NLA^OX^* plants was *c.* 5, whereas it is *c.* 2 in WT, indicating increased instability of PHR1 in *NLA^OX^* plants. By contrast, PHR1 protein levels in *nla* plants were higher than in WT in samples without MG132 and only a modest increase was seen with MG132 treatment (Fig. 4b). In the *nla* mutant, the ratio of PHR1 protein levels with and without MG132 was *c.* 1.25, whereas it is *c.* 2 in WT, indicating increased stability of PHR1 in the mutant. Control experiments showed no significant difference in *PHR1* and *NLA* transcript levels in WT, *nla* and *NLA^OX^* plants with and without MG132 treatment (Fig. 4d). We also measured the stability of PHR1 in WT, *nla* and *NLA^OX^* by cycloheximide-chase experiments.

Fig. 4(c) shows that PHR1 in *nla* remained stable for 9 h after cycloheximide addition. By contrast, 35% of PHR1 in WT and 75% of PHR1 in *NLA^OX^* were degraded in the same time period. These results show that the level and stability of PHR1 are inversely correlated with NLA levels, consistent with the notion that PHR1 is targeted by NLA for ubiquitination and degradation.

InsP6 enhances polyubiquitination of PHR1 by NLA E3 ligase

Previous reports demonstrated SPX domains contain a basic surface that is able to interact with InsP6. InsP7, which has a higher affinity for SPX domains than InsP6, stimulated the interaction between OsSPX4 and OsPHR2 (Wild *et al.*, 2016). Recently, InsP8 was found to be important for SPX1/PHR1 binding (Dong *et al.*, 2019). Because NLA contains an SPX domain in its N-terminal region that interacted with PHR1, we hypothesized that InsPn may regulate PHR1/NLA complex formation. To test

Fig. 5 InsP6 enhances ubiquitination of PHOSPHATE STARVATION RESPONSE 1 (PHR1) mediated by NITROGEN LIMITATION ADAPTATION (NLA). (a) InsP6 increases the association of PHR1 with NLA *in vitro*. One microgram of resin-bound GST-PHR1 was mixed with 2 μg of MBP-NLA or MBP-SPX and with different amounts (0–40 μM) of InsP6. MBP-NLA or MBP-SPX associated with GST-PHR1 was detected by anti-MBP antibody (top panel). The gel blot was stained with Coomassie brilliant blue (bottom panel). MBP-NLA and MBP-SPX in the first lane were used as positive controls. (b) InsP6 increases the ubiquitination of PHR1 mediated by NLA. MBP-PHR1-myc was mixed with yeast UBE1 (E1), human UBCH6E1 (E2), MBP-NLA-HA (E3) and different amounts (0–10 μM) of InsP6 or InsP5. Ubiquitinated MBP-PHR1-myc was detected by anti-myc antibody.

this hypothesis, we performed *in vitro* pull-down assays with different amounts of InsP6 because InsP7 and InsP8 are not commercially available. Fig. 5(a) shows that NLA binding to PHR1 was indeed enhanced by increasing amounts of InsP6. Similar effects of InsP6 were obtained with the NLA SPX domain alone.

Next, we performed *in vitro* ubiquitination assay to determine whether InsP6 can facilitate PHR1 ubiquitination since it enhances NLA/PHR1 complex formation. Fig. 5(b) shows that polyubiquitination of PHR1 was enhanced by increasing InsP6 concentrations and the effect was saturated at 10 μM InsP6 (Fig. S3). By contrast, there was no difference in the polyubiquitination pattern of PHR1 with InsP5 addition (Fig. 5b).

Dynamic changes in gene expression and PHR1/NLA protein levels during +Pi to −Pi transition

We performed a time-course study to gain insight into dynamic changes in NLA and PHR1 levels and PSR gene expression during Pi starvation. Ten-day-old seedlings grown on +Pi medium were transferred to −Pi medium, and daily samples were collected for protein and RNA analysis for 7 d. We monitored transcript levels of five PSR genes: *IPS1*, *AT4*, *ANS*, *pri-mi399d* and *pri-miR827* as well as *PHO2* and *NLA*, which are targets of *miR399d* and *miR827*, respectively. *PHO2* encodes UBC24, which is the cognate E2 for NLA E3 ligase (Park *et al.*, 2018) and which we have shown to be active in mediating PHR1 ubiquitination *in vitro* (Fig. S2). Fig. 6 shows that PSR genes were activated on Day 2 after transfer and transcript levels of all five PSR genes increased steadily to Day 7. The decrease in *PHO2* transcript basically paralleled the increase

in *pri-miR399d*. In the case of *NLA*, transcript levels decreased by 30% on Day 1 when there was little expression of *pri-miR827*. However, from Days 2 to 7, *NLA* transcript levels also showed an anti-correlation with *pri-miR827* levels. On Day 7, *NLA* transcript levels were reduced to *c.* 30% of those on Day 0. Transcript levels of *PHR1*, which encodes the major positive activator of PSR genes, did not change for 7 d following the transition to −Pi medium (Fig. 6a). These results suggest the importance of post-translational regulation of PHR1 in PSR. To investigate this issue, we used anti-NLA and anti-PHR1 antibodies to determine PHR1 and NLA protein levels following the −Pi transition. After 7 d on −Pi medium, NLA levels declined steadily to a residual value of *c.* 30% consistent with its transcript levels at this time point. By contrast, PHR1 levels increased steadily to about 2.3-fold on Day 3 to 2.8-fold on Days 6 and 7. The inverse relationship between PHR1 levels and NLA levels is consistent with our finding that PHR1 is degraded by NLA.

Since the PHR1/NLA association is also regulated by InsPn whose levels decreased with Pi starvation, we checked the status of PHR1/NLA complex in seedlings grown under −P conditions. Fig. 3(b) shows the presence of PHR1/NLA complex in seedlings grown in +Pi medium, but this complex was undetected in seedlings grown under −Pi (Fig. 6c). However, PHR1/NLA complex formation could be reconstituted *in vitro* upon the addition of InsP6 to the extracts of seedlings grown under −Pi medium, suggesting that InsPn may be limiting the interaction *in vivo* (Fig. 6d). Our results suggest that under −Pi conditions, the low InsPn levels allow dissociation of the PHR1/NLA complex to release PHR1 to activate downstream PSR genes.
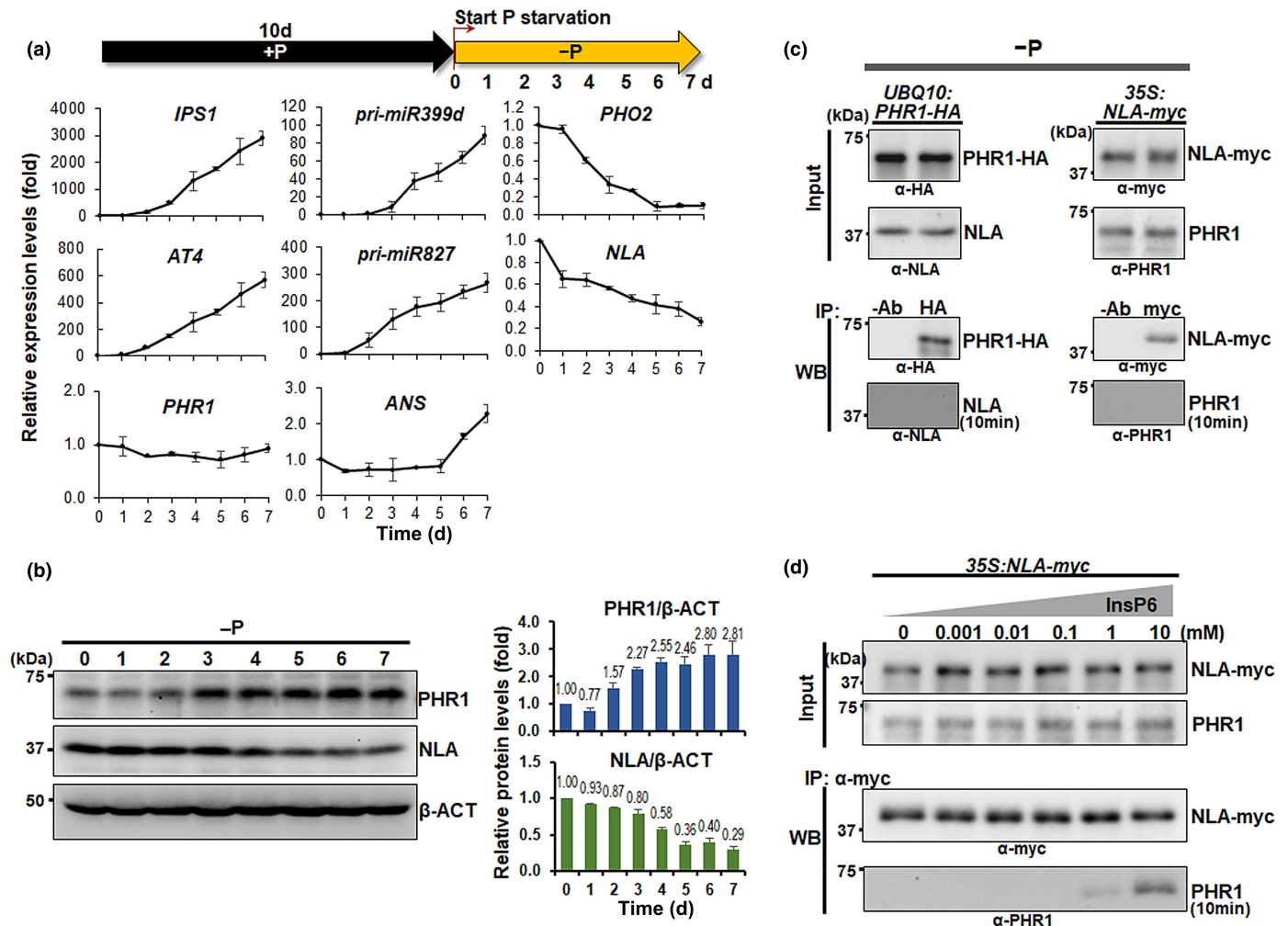
Fig. 6 Gene expression dynamics in WT plants in response to phosphate (Pi) starvation. (a) Ten-day-old seedlings of WT were transferred onto Pi-deficient (−P) medium. Seedlings were collected at the indicated days for 7 d. Transcript levels of Pi-starvation response genes (*IPS1*, *AT4*, *pri-miR827*, *pri-miR399d* and *anthocyanidin synthase*), *PHO2*, NITROGEN LIMITATION ADAPTATION (*NLA*) and PHOSPHATE STARVATION RESPONSE 1 (*PHR1*) were analysed by RT-qPCR. *ACT2* levels were used as an internal control. Bars are average values ±SD ($n = 3$, independent biological replicates). (b) PHR1 and NLA protein levels under −P conditions. Protein levels of PHR1 and NLA were detected by using anti-PHR1 and anti-NLA antibodies (left panel). β-ACT levels were used as a loading control. The intensity of the bands was measured using IMAGEJ and normalized by β-ACT levels (right panel). Values in sample 0 d set as 1. Bars are average values ±SD ($n = 3$, independent biological replicates). (c) PHR1 is unable to interact with NLA in Arabidopsis under −P conditions. Seedling of *UBQ10:PHR1-HA* and *35S:NLA-myc* were grown 10 d on MS medium and then transferred onto Pi-deficient (−P) medium for 7 d. Extracts were prepared from seedlings that were treated with 50 μM MG132 for 16 h. Left panel: Immunoprecipitates obtained with anti-HA antibody were tested for the presence of NLA-myc and NLA using anti-myc and anti-NLA antibodies. Right panel: Immunoprecipitates obtained with anti-myc antibody were tested for the presence of PHR1-HA and PHR1 using anti-HA and anti-PHR1 antibodies. IP, immunoprecipitation; −Ab, no antibody. Blots were exposed for 1 min, but the bottom blots of IP were exposed for 10 min. (d) Co-Immunoprecipitations analysis of *in vivo* interaction between PHR1 and NLA depending on different concentrations of InsP6. The seedlings of *35S:NLA-myc* were grown on +P medium for 10 d and then transferred to −P medium for 7 d. The seedlings were treated with 50 μM MG132 for 16 h before extraction. Different concentrations of InsP6 were added to the protein extraction. Immunoprecipitates obtained with anti-myc antibody were tested for the presence of PHR1 using anti-PHR1 antibody. Blots were exposed for 1 min, but the last blot was exposed for 10 min.

PHR1 levels in InsPn-related mutant and overexpression plants

Previous reports showed levels of InsP6, InsP7 and InsP8 are reduced in *itpk4-1* mutants, and contents of InsP6, InsP7 and InsP8 are increased in their overexpression lines (Kuo *et al.*, 2014, 2018). To investigate the effects of InsPn levels on PHR1 stability *in vivo*, we measured the half-life of PHR1 in WT, *itpk4-1* and *ITPK4^{OX}* by cycloheximide-chase experiments. Fig. 7(a) shows

that PHR1 in *ITPK4^{OX}* was degraded rapidly compared with that in WT. By contrast, PHR1 degradation pattern in *itpk4-1* was opposite to that of their overexpression plants. In Arabidopsis, InsP7 can be converted to InsP8 by VIH1/VIH2 (Dong *et al.*, 2019; Zhu *et al.*, 2019). To see whether InsP8 is essential for NLA and PHR1 interaction *in vivo*, we treated *vih2-4/VIH1^{amiRNA}* plants (Zhu *et al.*, 2019) with beta-oestradiol inducer to knock down the expression of *VIH1*. Upon inducer treatment of *vih2-4/VIH1^{amiRNA}* plants showed a 2.57-fold induction of
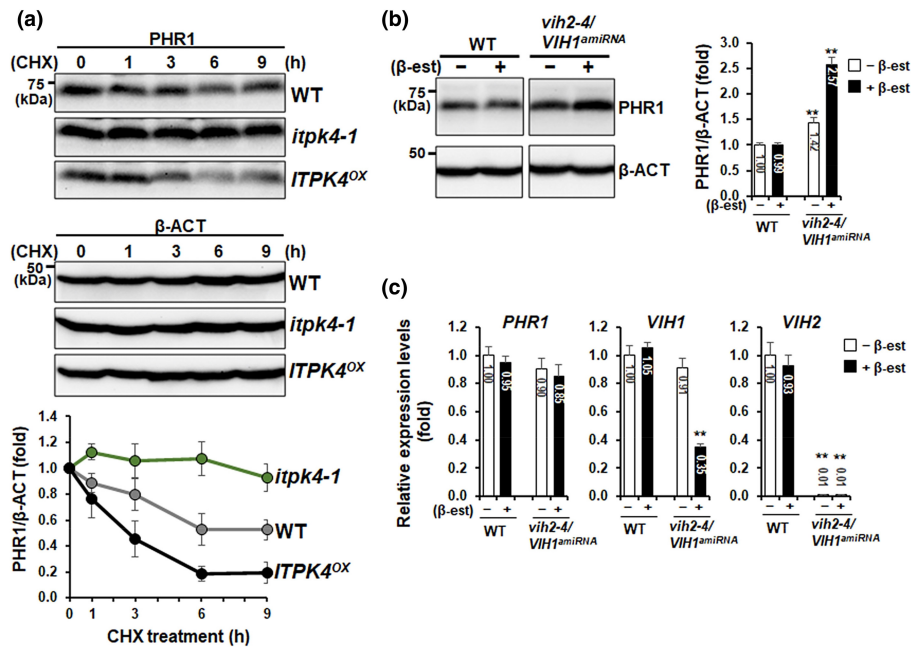
Fig. 7 PHOSPHATE STARVATION RESPONSE 1 (PHR1) levels in InsPn-related mutant and overexpression plants. PHR1 stability in InsPn-related mutants and overexpression plants. (a) The *itpk4-1* are loss-of-function mutants of encoded an *Inositol tetrakisphosphate-1 kinase* (*ITPK4*). InsP6 is deficient in mutants, whereas InsP3 is accumulated in *itpk4-1* (Kuo *et al.*, 2018). Ten-day-old seedlings of WT, *itpk4-1* and *ITPK4*^{OX} were treated in liquid Murashige and Skoog (MS) medium with 200 μM cycloheximide (CHX). Proteins were extracted at indicated times and analysed by immunoblots using anti-PHR1 and anti-β-actin antibodies (upper panel). β-actin levels were used as a loading control and the intensity of the PHR1 protein bands was measured using IMAGEJ and normalized by β-actin levels (lower panel). Values in sample 0 time were set as 1. Plots are average values ±SD (*n* = 3, independent biological replicates). (b) PHOSPHATE STARVATION RESPONSE 1 protein levels in *vih2-4/VIH1*^{amiRNA} plants. Ten-day-old seedlings of WT and *vih2-4/VIH1*^{amiRNA} were incubated in liquid Murashige and Skoog medium with or without β-oestradiol (10 μM) for 22 h, and extracts were prepared. PHR1 proteins were detected using anti-PHR1 antibody, and β-actin was used as a loading control (left panel). The intensity of protein bands was measured using IMAGEJ, and numbers indicate relative values ±SD (right panel) (*n* = 3, independent biological replicates). (c) Analysis of *PHR1*, *VIH1* and *VIH2* transcript levels in (b). Transcript levels were analysed by qRT-PCR and normalized to *ACT2* levels. Bars represent average values ±SD (*n* = 3, independent biological replicates). Asterisks indicate a statistically significant difference compared with WT. **, *P* < 0.01; two-tailed *t*-test.

PHR1 protein levels compared with WT (Fig. 7b). Control experiments showed no detectable changes in *PHR1* transcript levels (Fig. 7c). Taken together, our results suggest InsP8 and InsP6 can promote PHR1 instability *in vivo* by enhancing the association of PHR1 with its cognate NLA E3 ligase.

Discussion

The MYB transcription factor, PHR1, was first identified by Rubio *et al.* (2001) as a central regulator for PSR more than two decades ago. The initial finding that *PHR1* transcript levels were only marginally responsive to Pi levels in the medium (Rubio *et al.*, 2001) has since been confirmed by others (Klecker *et al.*, 2014) and by our results (Fig. 6) reported here. The apparent lack of transcriptional regulation of *PHR1* suggests that PSR likely entails post-translational regulation of the PHR1 protein and its abundance. Here, we have identified the NLA E3 ligase as the negative regulator of PHR1 protein levels in PSR. Several lines of evidence support our claim: (1) Plants of *nla* mutant have similar morphological phenotype compared with *PHR1* overexpression plants showing constitutive PSR whereas *NLA* overexpression plants phenocopy *phr1* mutant. (2) The morphological changes in these plants are accompanied by the expected changes in PSR-related gene expression. (3) NITROGEN LIMITATION

ADAPTATION forms a complex with PHR1 *in vitro* and *in vivo*. (4) NITROGEN LIMITATION ADAPTATION can target PHR1 for polyubiquitination *in vitro*. (5) Compared with WT, PHR1 levels are higher in *nla* mutant but lower in *NLA* overexpression plants, indicating negative regulation of PHR1 protein levels by NLA.

Initially identified as a positive regulator of a plant's responses to nitrogen limitation conditions (Peng *et al.*, 2007), NLA was subsequently implicated in PSR as well (Kant *et al.*, 2011). Like other RING-motif proteins, NLA possesses E3 ligase activity suggesting its potential role in downregulating target protein abundance. NITROGEN LIMITATION ADAPTATION transcript levels are targeted for cleavage by *miRNA827*, which is transcriptionally induced by Pi depletion. Under +P conditions, there is no induction of *miR827* and NLA interacts with membrane-bound Pi transporters through its SPX domain and marks these transporters for ubiquitination and degradation (Lin *et al.*, 2013; Park *et al.*, 2014). By contrast, the induction of *miR827* under −P conditions (Hsieh *et al.*, 2009; Kant *et al.*, 2011) reduces *NLA* transcript and protein levels, thus decreasing the continuous degradation of the Pi transporters and allowing their stable accumulation. These results with Pi transporters suggest that the negative regulation of PHR1 by NLA likely involves ubiquitination and degradation as well. Indeed, we showed here that NLA uses
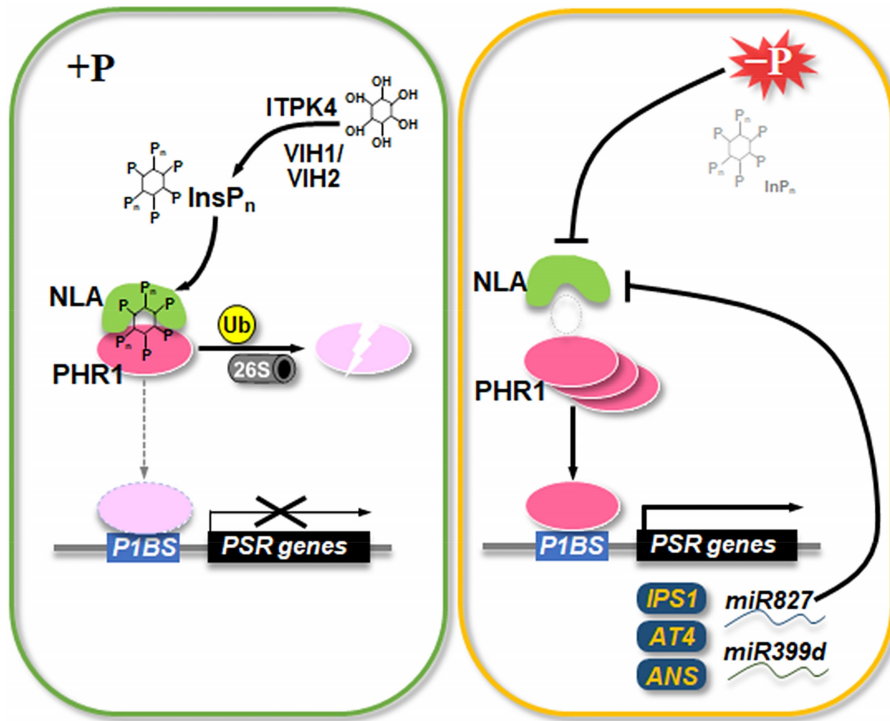
Fig. 8 Model for PHOSPHATE STARVATION RESPONSE 1 (PHR1) regulation mediated by NITROGEN LIMITATION ADAPTATION (NLA) E3 ligase in plants. Inositol polyphosphate kinases (ITPK; e.g. ITPK4 and VIH1/VIH2) biosynthesize InsP6, InsP7 and InsP8 through a series of sequential reactions. The InsPn molecule accumulated in the cell promotes the binding of PHR1 and NLA, and PHR1 is ubiquitinated by NLA E3 ligase activity and eventually degraded by the 26S proteasome. Destabilization of PHR1 does not induce phosphate (Pi) starvation response (PSR) genes (grey-dashed arrows). On the contrary, as the intracellular InsPn concentration decreases during Pi starvation, the PHR1-NLA interaction weakens, releasing PHR1 from NLA. The stabilized PHR1 protein activates transcription of downstream PSR genes. One of these downstream genes, *pri-miR827*, produces mature *miR827* which targets the cleavage of *NLA* transcripts and reduces its expression levels.

its SPX domain to bind to PHR1 and to polyubiquitinate the transcription factor in an SPX-dependent manner *in vitro*.

Plant stand-alone SPX domain proteins have been shown to be important sensors of intracellular Pi status (Wang *et al.*, 2009, 2014; Lv *et al.*, 2014; Puga *et al.*, 2014; Ried *et al.*, 2021). Under Pi-replete conditions, AtSPX1 sequesters PHR1 and prevents it from accessing target gene promoters and the rice OsSPX4 similarly restrains OsPHR2 from activating downstream genes (Lv *et al.*, 2014; Puga *et al.*, 2014; Wang *et al.*, 2014). Recent reports showed intracellular Pi sensing is mediated by InsP6 and InsP7 that can enhance OsSPX4/OsPHR2 interaction (Wild *et al.*, 2016), and InsP8, which has the highest binding affinity to AtSPX1, can similarly promote AtSPX1/PHR1 complex formation (Dong *et al.*, 2019). These observations prompted us to examine the regulatory effects of (InsPn) on NLA/PHR1 binding and ubiquitination. Indeed, we found that NLA/PHR1 binding is promoted by InsP6 but not by InsP5 and that increased polyubiquitination *in vitro* is seen along with the enhanced interaction.

Our *in vitro* results on InsPn-regulated ubiquitination of PHR1 by NLA are supported by measurement of PHR1 protein half-life among WT and mutants with altered InsPn metabolism (Fig. 7). Mutant plants of *ipk1*, *itpk4* and *vih1/vih2* have been shown to be defective in sensing Pi (Kuo *et al.*, 2018; Dong *et al.*, 2019; Zhu *et al.*, 2019; Ried *et al.*, 2021). Under Pi-replete conditions, InsP6, InsP7 and InsP8 levels are reduced in *itpk4-1* mutants compared with WT, whereas levels of these InsPn should be elevated in *ITPK4^{OX}* plants. We found that PHR1 protein half-life is prolonged in the *itpk4-1* mutant but shortened in *ITPK4^{OX}* plants compared with WT (Fig. 7a). Moreover, *VIH1/VIH2* knock-down plants, *vih2-4/VIH1^{amiRNA}*, showed an increase in PHR1 levels resulting from a decrease in InsP8 levels

(Fig. 7b,c), providing evidence that InsP8 is essential for NLA-mediated PHR1 degradation *in vivo*. Our results are consistent with the view that InsPn (InsP6-8) promote NLA/PHR1 complex formation, increase PHR1 ubiquitination and accelerate PHR1 instability.

In seedlings, root hair length and shoot anthocyanin levels are determined by PHR1 levels (Zhou *et al.*, 2008; Bustos *et al.*, 2010; Sun *et al.*, 2016). We found that *nla* and *PHR1^{OX}* seedlings, which express high PHR1 levels, produce long root hair and that accumulate high levels of anthocyanin in shoots under −P conditions; by contrast, *NLA^{OX}* and *phr1* seedlings, which have little or no PHR1, display the opposite phenotypes (Figs 1, 2). The inverse relationship between NLA and PHR1 levels is further confirmed by a time-course experiment monitoring transcript and protein changes during the initial phase of Pi depletion (Fig. 6a,b). In confirmation of previous report, there is little change in *PHR1* transcript levels during Pi starvation. On the contrary, upon shifting from PI-sufficient to Pi-deficient medium, *pri-miR827* levels increase, whereas *NLA* transcript levels decrease (Fig. 6a). This inverse relationship between the two transcripts is consistent with the cleavage of *NLA* mRNA mediated by the induced *miR827* (Hsieh *et al.*, 2009; Kant *et al.*, 2011; Fig. 6). This decline in *NLA* transcript levels is in contrast with the fairly steady *PHR1* transcript levels during the first 7 d of PSR. Nonetheless, the analysis of protein levels shows an inverse relationship between NLA and PHR1 (Fig. 6b).

Collectively, our results can be best explained by the working model presented in Fig. 8. Under +P condition, InsPn levels are high, which enable the binding of the high levels of NLA to PHR1 and to mediate the destruction of the transcription factor by 26 S proteasomes. Upon shifting to −P medium, the

suppression of *NLA* transcript by *miR827* leads to reduced NLA protein levels. Moreover, the lower InsPn levels under −P conditions would favour the dissociation of the NLA/PHR1 complex (Fig. 6), thus allowing the accumulated PHR1 to activate downstream PSR genes.

Several reports have highlighted the importance of SPX domain in the interaction between components of several eukaryotic signalling pathways. The yeast SPL2 interacts with the SPX domain of PHO87 and PHO90 to inhibit Pi efflux under low Pi conditions (Hürlimann *et al.*, 2009). In Arabidopsis, PHO1 interacts with the SPX domain of PHO2 (Liu *et al.*, 2012) and the transcriptional coactivator SHORT HYPOCOTYL UNDER BLUE1 contains an SPX domain at its N-terminus which binds to MINI3 to regulate seed development process (Zhou *et al.*, 2009; Kang *et al.*, 2013). It would be interesting to investigate whether InsPn are also involved in the regulation of these interactions and pathways.

Acknowledgement

Author contributions

ORCID

Nam-Hai Chua https://orcid.org/0000-0002-8991-0355
Jin Seo Jeong https://orcid.org/0000-0002-8926-7793
Bong Soo Park https://orcid.org/0000-0001-6550-0995
Su-Hyun Park https://orcid.org/0000-0002-9237-7600

Data availability

The data that support the findings of this study are available from the corresponding author upon reasonable request.

References

Aung K, Lin S-I, Wu C-C, Huang Y-T, Su C-I, Chiou T-J. 2006. *pho2*, a phosphate overaccumulator, is caused by a nonsense mutation in a microRNA399 target gene. *Plant Physiology* 141: 1000–1011.

Bari R, Datt PB, Stitt M, Scheible WR. 2006. PHO2, microRNA399, and PHR1 define a phosphate-signaling pathway in plants. *Plant Physiology* 141: 988–999.

Barragán-Rosillo AC, Peralta-Alvarez CA, Ojeda-Rivera JO, Arzate-Mejía RG, Recillas-Targa F, Herrera-Estrella L. 2021. Genome accessibility dynamics in response to phosphate limitation is controlled by the PHR1 family of transcription factors in Arabidopsis. *Proceedings of the National Academy of Sciences, USA* 118: e2107558118.

Bieleski RL. 1973. Phosphate pools, phosphate transport, and phosphate availability. *Annual Review of Plant Physiology* 24: 225–252.

Bustos R, Castrillo G, Linhares F, Puga MI, Rubio V, Pérez-Pérez J, Solano R, Leyva A, Paz-Ares J. 2010. A central regulatory system largely controls transcriptional activation and repression responses to phosphate starvation in Arabidopsis. *PLoS Genetics* 6: e1001102.

Chen YF, Li LQ, Xu Q, Kong YH, Wang H, Wu WH. 2009. The WRKY6 transcription factor modulates PHOSPHATE1 expression in response to low Pi stress in Arabidopsis. *Plant Cell* 21: 3554–3566.

Clough SJ, Bent AF. 1998. Floral dip: a simplified method for Agrobacterium-mediated transformation of *Arabidopsis thaliana. The Plant Journal* 16: 735–743.

Cridland C, Gillaspy G. 2020. Inositol pyrophosphate pathways and mechanisms: what can we learn from plants? *Molecules* 25: 2789.

Devaiah BN, Nagarajan VK, Raghothama KG. 2007. Phosphate homeostasis and root development in Arabidopsis are synchronized by the zinc finger transcription factor ZAT6. *Plant Physiology* 145: 147–159.

Dong J, Ma G, Sui L, Wei M, Satheesh V, Zhang R, Ge S, Li J, Zhang TE, Wittwer C *et al.* 2019. Inositol pyrophosphate InsP8 acts as an intracellular phosphate signal in Arabidopsis. *Molecular Plant* 12: 1463–1473.

Franco-Zorrilla JM, González E, Bustos R, Linhares F, Leyva A, Paz-Ares J. 2004. The transcriptional control of plant responses to phosphate limitation. *Journal of Experimental Botany* 55: 285–293.

Fujiwara T, Hirai MY, Chino M, Komeda Y, Naito S. 1992. Effects of sulfur nutrition on expression of the soybean seed storage protein genes in transgenic petunia. *Plant Physiology* 99: 263–268.

Guo M, Ruan W, Li C, Huang F, Zeng M, Liu Y, Yu Y, Ding X, Wu Y, Wu Z *et al.* 2015. Integrative comparison of the role of the PHOSPHATE RESPONSE1 subfamily in phosphate signaling and homeostasis in rice. *Plant Physiology* 168: 1762–1776.

Guo M, Ruan W, Zhang Y, Zhang Y, Wang X, Guo Z, Wang L, Zhou T, Paz-Ares J, Yi K. 2022. A reciprocal inhibitory module for Pi and iron signaling. *Molecular Plant* 15: 138–150.

Hinsinger P. 2001. Bioavailability of soil inorganic P in the rhizosphere as affected by root-induced chemical changes: a review. *Plant and Soil* 237: 173–195.

Hsieh LC, Lin SI, Shih AC, Chen JW, Lin WY, Tseng CY, Li WH, Chiou TJ. 2009. Uncovering small RNA-mediated responses to phosphate deficiency in Arabidopsis by deep sequencing. *Plant Physiology* 151: 2120–2132.

Hürlimann HC, Pinson B, Stadler-Waibel M, Zeeman SC, Freimoser FM. 2009. The SPX domain of the yeast low-affinity phosphate transporter Pho90 regulates transport activity. *EMBO Reports* 10: 1003–1008.

Kandhol N, Singh VP, Herrera-Estrella L, Tran L-SP, Tripathi DK. 2022. Arsenite: the umpire of arsenate perception and responses in plants. *Trends in Plant Science* 27: 420–422.

Kang X, Li W, Zhou Y, Ni M. 2013. A WRKY transcription factor recruits the SYG1-like protein SHB1 to activate gene expression and seed cavity enlargement. *PLoS Genetics* 9: e1003347.

Kant S, Peng M, Rothstein SJ. 2011. Genetic regulation by NLA and microRNA827 for maintaining nitrate-dependent phosphate homeostasis in Arabidopsis. *PLoS Genetics* 7: e1002021.

Klecker M, Gasch P, Peisker H, Dörmann P, Schlicke H, Grimm B, Mustroph A. 2014. A shoot-specific hypoxic response of Arabidopsis sheds light on the role of the phosphate-responsive transcription factor PHOSPHATE STARVATION RESPONSE1. *Plant Physiology* 165: 774–790.

Kuo HF, Chang TY, Chiang SF, Wang WD, Charng YY, Chiou TJ. 2014. Arabidopsis inositol pentakisphosphate 2-kinase, AtIPK1, is required for growth and modulates phosphate homeostasis at the transcriptional level. *The Plant Journal* 80: 503–515.

Kuo HF, Hsu YY, Lin WC, Chen KY, Munnik T, Brearley CA, Chiou TJ. 2018. Arabidopsis inositol phosphate kinases IPK1 and ITPK1 constitute a metabolic pathway in maintaining phosphate homeostasis. *The Plant Journal* 95: 613–630.

Laby RJ, Kincaid MS, Kim D, Gibson SI. 2000. The Arabidopsis sugar-insensitive mutants sis4 and sis5 are defective in abscisic acid synthesis and response. *The Plant Journal* 23: 587–596.

Lin WY, Huang TK, Chiou TJ. 2013. Nitrogen limitation adaptation, a target of microRNA827, mediates degradation of plasma membrane-localized phosphate transporters to maintain phosphate homeostasis in Arabidopsis. *Plant Cell* 25: 4061–4074.

Liu TY, Huang TK, Tseng CY, Lai YS, Lin SI, Lin WY, Chen JW, Chiou TJ. 2012. PHO2-dependent degradation of PHO1 modulates phosphate homeostasis in *Arabidopsis*. *Plant Cell* **24**: 2168–2183.

Liu TY, Huang TK, Yang SY, Hong YT, Huang SM, Wang FN, Chiang SF, Tsai SY, Lu WC, Chiou TJ. 2016. Identification of plant vacuolar transporters mediating phosphate storage. *Nature Communications* **7**: 11095.

Lv Q, Zhong Y, Wang Y, Wang Z, Zhang L, Shi J, Wu Z, Liu Y, Mao C, Yi K et al. 2014. SPX4 negatively regulates phosphate signaling and homeostasis through its interaction with PHR2 in rice. *Plant Cell* **26**: 1586–1597.

Martín AC, del Pozo JC, Iglesias J, Rubio V, Solano R, de La Peña A, Leyva A, Paz-Ares J. 2000. Influence of cytokinins on the expression of phosphate starvation responsive genes in Arabidopsis. *The Plant Journal* **24**: 559–567.

Mitra GN. 2015. *Regulation of nutrient uptake by plants, vol. 10*. New Delhi, India: Springer, 978–981.

Navarro C, Mateo-Elizalde C, Mohan TC, Sánchez-Bermejo E, Urrutia O, Fernández-Muñiz MN, García-Mina JM, Muñoz R, Paz-Ares J, Castrillo G et al. 2021. Arsenite provides a selective signal that coordinates arsenate uptake and detoxification through the regulation of PHR1 stability in Arabidopsis. *Molecular Plant* **14**: 1489–1507.

Nilsson L, Müller R, Nielsen TH. 2007. Increased expression of the MYB-related transcription factor, PHR1, leads to enhanced phosphate uptake in *Arabidopsis thaliana*. *Plant, Cell & Environment* **30**: 1499–1512.

Park BS, Seo JS, Chua NH. 2014. NITROGEN LIMITATION ADAPTATION recruits PHOSPHATE2 to target the phosphate transporter PT2 for degradation during the regulation of Arabidopsis phosphate homeostasis. *Plant Cell* **26**: 454–464.

Park BS, Yao T, Seo JS, Wong ECC, Mitsuda N, Huang CH, Chua NH. 2018. *Arabidopsis* NITROGEN LIMITATION ADAPTATION regulates ORE1 homeostasis during senescence induced by nitrogen deficiency. *Nature Plants* **4**: 898–903.

Park SH, Jeong JS, Seo JS, Park BS, Chua NH. 2019. Arabidopsis ubiquitin-specific proteases UBP12 and UBP13 shape ORE1 levels during leaf senescence induced by nitrogen deficiency. *New Phytologist* **223**: 1447–1460.

Park SH, Jeong JS, Zhou Y, Mustafa NF, Chua NH. 2022. Deubiquitination of BES1 by UBP12/UBP13 promotes brassinosteroid signaling and plant growth. *Plant Communications* **3**: 100348.

Peng M, Hannam C, Gu H, Bi YM, Rothstein SJ. 2007. A mutation in NLA, which encodes a RING-type ubiquitin ligase, disrupts the adaptability of Arabidopsis to nitrogen limitation. *The Plant Journal* **50**: 320–337.

Puga MI, Mateos I, Charukesi R, Wang Z, Franco-Zorrilla JM, de Lorenzo L, Irigoyen ML, Masiero S, Bustos R, Rodríguez J et al. 2014. SPX1 is a phosphate-dependent inhibitor of phosphate starvation response 1 in Arabidopsis. *Proceedings of the National Academy of Sciences, USA* **111**: 14947–14952.

Ren F, Guo QQ, Chang LL, Chen L, Zhao CZ, Zhong H, Li XB. 2012. *Brassica napus* PHR1 gene encoding a MYB-Like protein functions in response to phosphate starvation. *PLoS ONE* **7**: e44005.

Ried MK, Wild R, Zhu J, Pipercevic J, Sturm K, Broger L, Harmel RK, Abriata LA, Hothorn LA, Fiedler D et al. 2021. Inositol pyrophosphates promote the interaction of SPX domains with the coiled-coil motif of PHR transcription factors to regulate plant phosphate homeostasis. *Nature Communications* **12**: 384.

Ruan W, Guo M, Wu P, Yi K. 2017. Phosphate starvation induced OsPHR4 mediates Pi-signaling and homeostasis in rice. *Plant Molecular Biology* **93**: 327–340.

Rubio V, Linhares F, Solano R, Martín AC, Iglesias J, Leyva A, Paz-Ares J. 2001. A conserved MYB transcription factor involved in phosphate starvation signaling both in vascular plants and in unicellular algae. *Genes & Development* **15**: 2122–2133.

Schachtman DP, Reid RJ, Ayling SM. 1998. Phosphorus uptake by plants: from soil to cell. *Plant Physiology* **116**: 447–453.

Stefanovic A, Ribot C, Rouached H, Wang Y, Chong J, Belbahri L, Delessert S, Poirier Y. 2007. Members of the *PHO1* gene family show limited functional redundancy in phosphate transfer to the shoot, and are regulated by phosphate deficiency via distinct pathways. *The Plant Journal* **50**: 982–994.

Su T, Xu Q, Zhang FC, Chen Y, Li LQ, Wu WH, Chen YF. 2015. WRKY42 modulates phosphate homeostasis through regulating phosphate translocation and acquisition in Arabidopsis. *Plant Physiology* **167**: 1579–1591.

Sun L, Song L, Zhang Y, Zheng Z, Liu D. 2016. Arabidopsis PHL2 and PHR1 act redundantly as the key components of the central regulatory system controlling transcriptional responses to phosphate starvation. *Plant Physiology* **170**: 499–514.

Tsui MM, York JD. 2010. Roles of inositol phosphates and inositol pyrophosphates in development, cell signaling and nuclear processes. *Advances in Enzyme Regulation* **50**: 324–337.

Wang C, Huang W, Ying Y, Li S, Secco D, Tyerman S, Whelan J, Shou H. 2012. Functional characterization of the rice SPX-MFS family reveals a key role of OsSPX-MFS1 in controlling phosphate homeostasis in leaves. *New Phytologist* **196**: 139–148.

Wang C, Ying S, Huang H, Li K, Wu P, Shou H. 2009. Involvement of OsSPX1 in phosphate homeostasis in rice. *The Plant Journal* **57**: 895–904.

Wang J, Sun J, Miao J, Guo J, Shi Z, He M, Chen Y, Zhao X, Li B, Han F et al. 2013. A phosphate starvation response regulator Ta-PHR1 is involved in phosphate signalling and increases grain yield in wheat. *Annals of Botany* **111**: 1139–1153.

Wang Y, Zhao X, Wang L, Jin S, Zhu W, Lu Y, Wang S. 2016. A five-year P fertilization pot trial for wheat only in a rice-wheat rotation of Chinese paddy soil: interaction of P availability and microorganism. *Plant and Soil* **399**: 305–318.

Wang Z, Ruan W, Shi J, Zhang L, Xiang D, Yang C, Li C, Wu Z, Liu Y, Yu Y et al. 2014. Rice SPX1 and SPX2 inhibit phosphate starvation responses through interacting with PHR2 in a phosphate-dependent manner. *Proceedings of the National Academy of Sciences, USA* **111**: 14953–14958.

Wild R, Gerasimaite R, Jung JY, Truffault V, Pavlovic I, Schmidt A, Saiardi A, Jessen HJ, Poirier Y, Hothorn M et al. 2016. Control of eukaryotic phosphate homeostasis by inositol polyphosphate sensor domains. *Science* **352**: 986–990.

Yi K, Wu Z, Zhou J, Du L, Guo L, Wu Y, Wu P. 2005. OsPTF1, a novel transcription factor involved in tolerance to phosphate starvation in rice. *Plant Physiology* **138**: 2087–2096.

Zhang X, Henriques R, Lin SS, Niu QW, Chua N-H. 2006. Agrobacterium-mediated transformation of *Arabidopsis thaliana* using the floral dip method. *Nature Protocols* **1**: 641–646.

Zhou J, Jiao F, Wu Z, Li Y, Wang X, He X, Zhong W, Wu P. 2008. OsPHR2 is involved in phosphate-starvation signaling and excessive phosphate accumulation in shoots of plants. *Plant Physiology* **146**: 1673–1686.

Zhou Y, Zhang X, Kang X, Zhao X, Zhang X, Ni M. 2009. SHORT HYPOCOTYL UNDER BLUE1 associates with *MINISEED3* and *HAIKU2* promoters in vivo to regulate *Arabidopsis* seed development. *Plant Cell* **21**: 106–117.

Zhu J, Lau K, Puschmann R, Harmel RK, Zhang Y, Pries V, Gaugler P, Broger L, Dutta AK, Jessen HJ et al. 2019. Two bifunctional inositol pyrophosphate kinases/phosphatases control plant phosphate homeostasis. *eLife* **8**: e43582.

Supporting Information

Additional Supporting Information may be found online in the Supporting Information section at the end of the article.

Fig. S1 Specificity of PHR1 antibody.

Fig. S2 PHR1 is ubiquitinated by NLA using PHO2 as an E2 enzyme.

Fig. S3 Higher InsP6 levels do not increase levels of polyubiquitinated PHR1 mediated by NLA.

Table S1 Primer list.

Please note: Wiley is not responsible for the content or functionality of any Supporting Information supplied by the authors. Any queries (other than missing material) should be directed to the *New Phytologist* Central Office.